Short communication

Suppression of Li deposition on surface of graphite using carbon coating by thermal vapor deposition process

Gumjae Park [a], Nanda Gunawardhana [a], Hiroyoshi Nakamura [a], YunSung Lee [b], Masaki Yoshio [a],*

[a] Department of Applied Chemistry, Saga University, 1 Honjo, Saga City, Saga 840-8502, Japan
[b] Faculty of Applied Chemical Engineering, Chonnam National University, 300 Yongbong-dong, Gwangju 500-757, Republic of Korea

ABSTRACT

10 wt.% carbon-coated natural graphite (NC-10) is prepared by thermal vapor deposition. The carbon coating is electrochemically investigated at $-5\,°C$; it improves lithium intercalation in the graphite's interlayer spacing. NC-10 graphite clearly shows 3 voltage plateaus and a higher capacity during the first charge/discharge cycle at $-5\,°C$ than uncoated natural graphite. XRD study of the electrode after the first charging shows increased lithium intercalation into the graphite layers and also suppression of lithium deposition on the graphite's surface. Due to the homogeneous potential profile on the graphite surface, carbon coating enhance lithium intercalation at $-5\,°C$. In addition, NC-10 shows less lithium deposition on the surface than bare natural graphite.

© 2011 Elsevier B.V. All rights reserved.

1. Introduction

Graphite is one of the most commonly used anodes materials in lithium ion batteries due to its low cost, low and flat working voltage, relatively high capacity of $372\,mAh\,g^{-1}$ and Coulombic efficiency in proper electrolyte [1]. However, it has irreversible capacity during its first charging due to the formation of SEI film and exfoliation caused by sensitivity to most PC-based electrolytes [2–4]. The introduction of additives to the electrolyte and the carbon coating of graphite electrode surfaces have been studied to overcome these disadvantages [5–13]. Different electrolyte additives decompose and produce different SEI films prior to the decomposition of the electrolyte. A suitable SEI film could prevent the exfoliation of the graphite and improve its electrochemical properties [5–9]. The carbon coating of graphite has also been studied to prevent exfoliation and reduce irreversible capacity during initial cycling [10–13]; it has been achieved by thermal vapor decomposition (TVD) in attempts to improve electrode performance [13–16]. Carbon-coated graphite has hybrid characteristics that can overcome most of the graphite's drawbacks while maintaining the benefits of the constituent graphite and carbon. Graphite coated with carbon has shown better electrochemical performance as an anode than natural graphite in both propylene carbonate and ethylene carbonate-based electrolytes.

In addition to the exfoliation that occurs in PC-based electrolyte, graphite electrodes also perform poorly at low temperature [17–24]. At temperatures below $0\,°C$, the electrochemical properties of graphite have been reported to deteriorate rapidly, allowing lithium deposition on the electrode's surface – a severe safety problem [25,26]. This occurs due to the low ionic conductivity of the electrolyte, the low diffusivity of lithium ions within the graphite, the high polarization of the graphite, and the high charge-transfer resistance of the electrolyte–electrode interfaces.

The introduction of 1,3-propane sultone electrolyte additive has been reported to improve electrochemical properties and reduce the formation of lithium dendrite on graphite surfaces at low temperature [26]. The surface modification of graphite with carbon is also thought to benefit graphite's electrochemical properties and suppress lithium dendrite formation on graphite surfaces at temperatures below $0\,°C$.

This work reports the TVD preparation of 10 wt.% carbon-coated natural graphite (NC-10). The effect of carbon coating was investigated by electrochemical testing at $-5\,°C$ of initial charge/discharge cycling. The suppression of lithium dendrite formation on the graphite surface and lithium intercalation in the graphene layers at $-5\,°C$ were observed by ex situ XRD measurement.

2. Experimental

10 wt.% carbon-coated natural graphite was prepared by a previously described TVD process [13]. Powder X-ray diffraction (XRD, Rint 1000, Rigaku, Japan) using CuKα radiation identified the mate-

* Corresponding author. Tel.: +81 952 20 4729; fax: +81 952 20 4729.
E-mail address: yoshio@cc.saga-u.ac.jp (M. Yoshio).

Fig. 1. XRD results of (a) natural graphite and (b) NC-10.
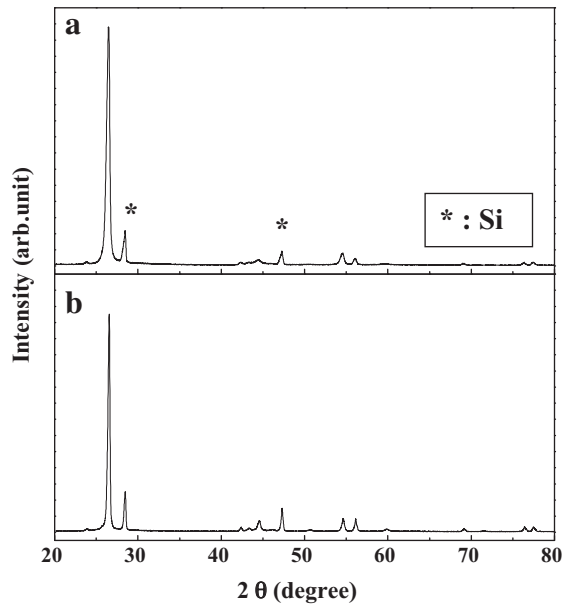

Fig. 3. Cyclic voltammograms of (a) natural graphite and (b) NC-10 in an electrolyte of $LiPF_6$ dissolved in EC-DEC (3:7 by volume) at −5 °C.

rials' crystalline phases. Particle morphologies were observed by scanning electron microscopy (SEM, S-4000, Hitachi Co., Japan). Electrochemical reactions of bare NG and NC-10 graphite were studied by cycle voltammetry (CV) in glass cells with 3 electrodes. The graphite electrode served as the working electrode and lithium metal foil was used as the counter and reference electrodes in 1.0 M $LiPF_6$-EC/DEC (3:7 vol.). The charge and discharge characteristics of the graphite electrode were examined in a screw-type cell comprising a lithium metal electrode (Cyprus Foote Mineral Co.) and a graphite electrode separated by 2 glass fibers. The graphite electrode was prepared from 90 wt.% graphite powder and 6 wt.% acetylene black suspended in an aqueous solution of 4 wt.% carboxymethylcelluose (CMC), which was spread on a copper foil current collector, dried at 100 °C, pressed at 150 kg cm^{-2}, and finally dried in a glass tube oven at 160 °C for 4 h. The charge and discharge current densities were 0.1 mA cm^{-2} with cut-off voltages from 0.005 V to 2.5 V.

Lithium deposition on the graphite surface after lithiation of the graphite layers was assessed by *ex- situ* X-ray diffractometry (XRD, MINIFlex Π, Rigaku, Japan) using CuKα radiation. The cells were
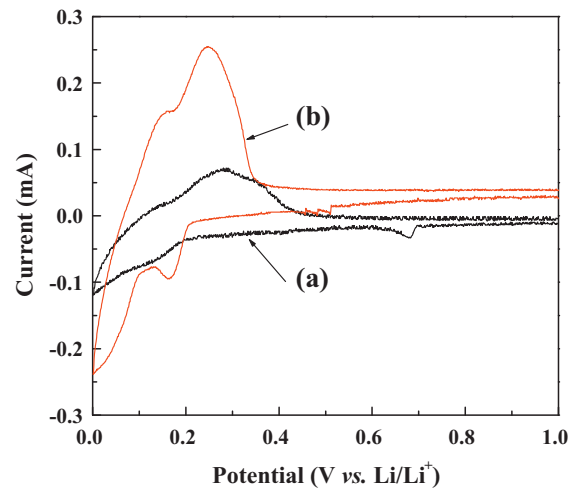
charged to 0.005 V at a current density of 0.1 mA cm^{-2}, and then maintained at 0.005 V for 10 h. The cells were disassembled and the electrodes were sealed in vinyl bags in an argon-filled glove box to prevent any reaction with moisture in the air.

3. Results and discussion

Fig. 1 shows the XRD patterns of NG and NC-10 graphite. Two graphite samples are highly crystallized. The (0 0 2) peaks at $2\theta = 26.55$ and 26.52° correspond to $d_{(0\,0\,2)}$ values of 3.354 and 3.558 Å for the natural graphite and NC-10, respectively. NC-10 showed a lower (0 0 2) peak intensity than the natural graphite due to the carbon coating. The degrees of graphitization were 99.1% and 94.1% for NG and NC-10 graphite, respectively. The respective contents of rhombohedral phase in the samples were 30.9% and 17.3%. Carbon coating decreased the presence of rhombohedral phase because the process involved heat treatment [27,28]. The XRD confirm that both graphite samples were highly crystalline graphite.

SEM images (Fig. 2) show that the natural graphite comprised flake-like particles of 10–30 μm. NC-10 contained circular carbon particles deposited on the graphite particles. The shapes of the NG particles changed to show only the curved planes of the carbon coating, indicating that the NG was fully covered with carbon [15].
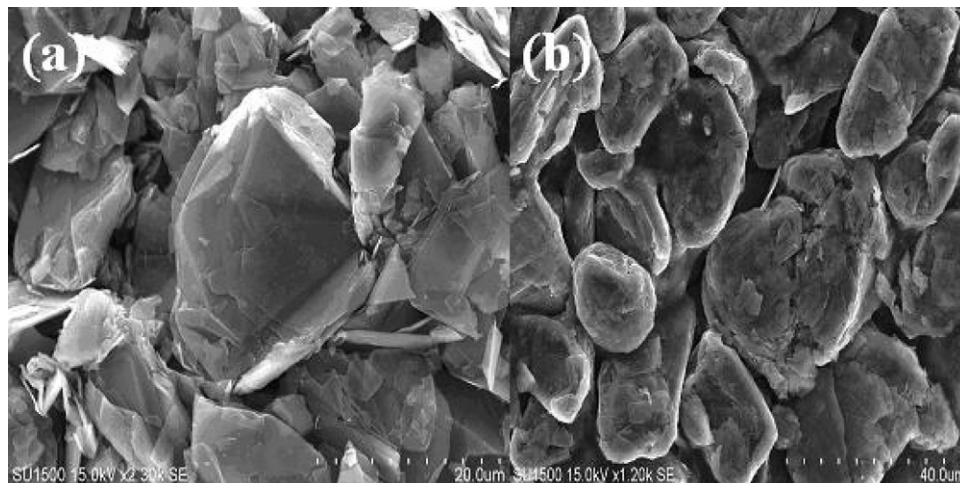

Fig. 2. SEM images of (a) natural graphite and (b) NC-10.

Fig. 3 presents that cyclic voltammetry demonstrated the effects of carbon coating on the graphite. Typical cyclic voltammograms of the graphite samples were measured in an electrolyte of 1 M $LiPF_6$-EC/DEC (3:7 by volume) at $-5\,°C$. The NG electrode showed only two couples of reversible redox peaks below 0.3 V vs. Li/Li^+ at $-5\,°C$, whereas it usually exhibit three couples of reversible redox peaks at room temperature. The reversible peaks are due to the reversible stage transformation between Li and graphite intercalation compounds [14,29]. The currents were also very small due to the low intercalation of lithium ions and difficulty of their diffusion in the graphene layers. NC-10 graphite clearly exhibited two reduction and oxidation peaks. Although both samples showed anodic peaks below 0.2 V and cathodic peak below 0.4 V, the higher anodic and cathodic peaks of NC-10 are indicative of its higher capacity than that of the NG. Therefore, NC-10 was expected to show better electrochemical properties at low temperature than NG due to the surface modification. The nature of the graphite's surface affects the formation of SEI film during charging and discharging [17]. NC-10 was expected to be able to form more effective SEI film and also enhance lithium diffusion into the graphite at $-5\,°C$.

Fig. 4 shows the first charge/discharge curves of NG/Li and NC-10/Li cells at $-5\,°C$ (current density: $0.1\,mA\,cm^{-2}$, cut-off voltage: 2500–5 mV) in an electrolyte of 1 M $LiPF_6$-EC/DEC (3:7 by volume). NG showed voltage plateaus at ca. 150 and 65 mV that decreased to 5 mV during charging. Plateaus at ca. 180 mV and 275 mV were observed during discharge. The 3 voltage plateaus observed at room temperature indicate stage changes due to lithium intercalation into the graphite during charging. The NG/Li cell cycled at $-5\,°C$ showed only 2 voltage plateaus during charging. The Li–intercalated graphite compound did not form the 1st stage of LiC_6 because of the low level of lithium intercalation into the graphene layers. Intercalation and extraction of Li ions were expected to be slower at $-5\,°C$ than that at $25\,°C$. NG showed a charge capacity of $225\,mAh\,g^{-1}$, a discharge capacity of $202\,mAh\,g^{-1}$, and therefore, an irreversible capacity of $23\,mAh\,g^{-1}$ during the first cycle. NC-10 graphite showed three plateaus at 180, 65, and 25 mV during charging and three at 125, 180, and 250 mV during discharge. The voltage plateaus of NC-10 during charging occurred at higher voltages than those of the natural graphite, indicating that the carbon coating affected the electrochemical properties. Coating improved the conductivity of the graphite's surface and its layers; it also reduced resistance between the graphite's
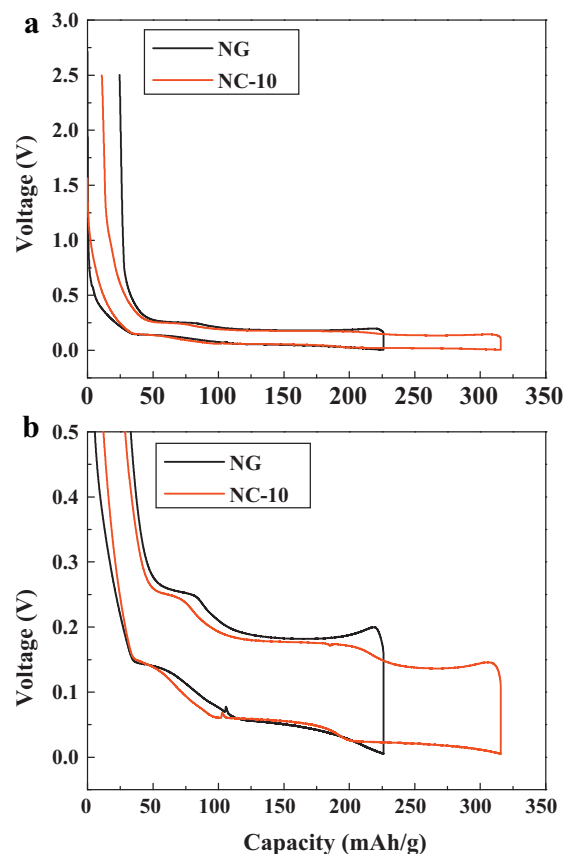

Fig. 4. (a) The first charge/discharge curves of natural graphite and NC-10 in an electrolyte of $LiPF_6$ dissolved in EC-DEC (3:7 by volume) at $-5\,°C$, and (b) magnification of graph (a) in the voltage region from OCV to 5 mV.

surface and the electrolyte. NC-10 also exhibited higher charge and discharge capacities (320 and $301\,mAh\,g^{-1}$, respectively) and an irreversible capacity of $25\,mAh\,g^{-1}$. Lithium ions could more easily intercalate into the NC-10 at $-5\,°C$ than into NG.

Fig. 5 shows images of the natural graphite and NC-10 after the first charge at $-5\,°C$. NG appeared black with some yellow
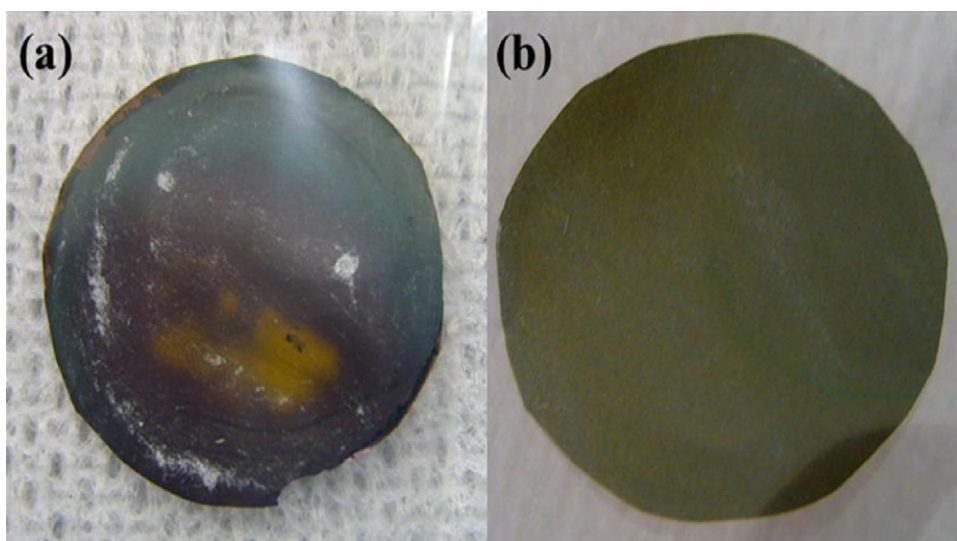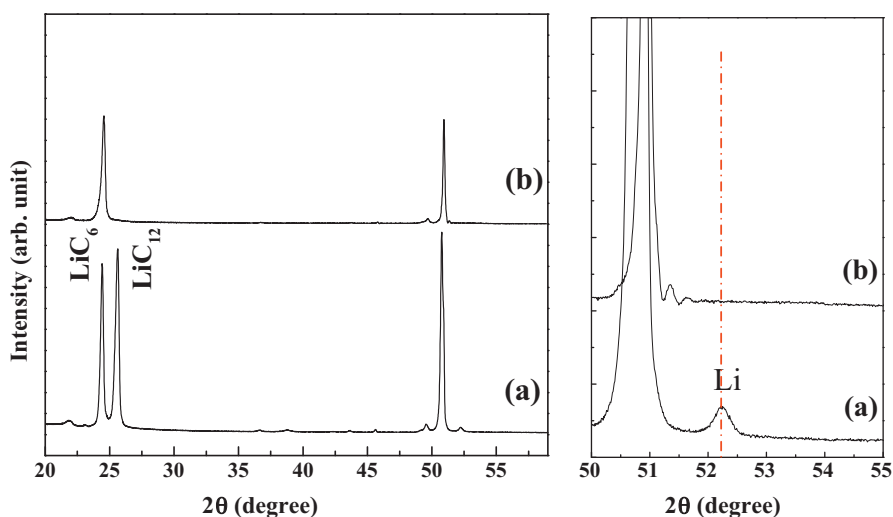

Fig. 5. Photographs of (a) natural graphite and (b) NC-10 after the first charging in an electrolyte of $LiPF_6$ dissolved in EC-DEC (3:7 by volume). The test conditions were one charging to 5 mV at a current density of $0.1\,mA\,cm^{-2}$ and holding at 5 mV for 10 h at $-5\,°C$.

Fig. 6. XRD results of (a) natural graphite and (b) NC-10 in an electrolyte of LiPF$_6$ dissolved in EC-DEC (3:7 by volume) after the first charge. The test conditions were one charging to 5 mV at a current density of 0.1 mA cm^{-2} and holding at 5 mV for 10 h at −5 °C.

areas (For interpretation of the references to colour in this figure text, the reader is referred to the web version of this article.). Previous work suggests that the black color indicates the formation of LiC$_{12}$ and lithium deposition on the surface of the graphite. The yellow color indicates the formation of first stage LiC$_6$ due to lithium intercalation into the graphene layers [29]. NC-10 appeared mainly yellow with some small areas of black. The carbon coating appeared to improve lithium diffusion in the graphite through a modified SEI film, which suppressed lithium dendrite formation.

Ex-situ XRD verified the effects of carbon coating on lithium deposition on the graphite. Fig. 6 shows *ex-situ* XRD results of: (a) natural graphite and (b) NC-10 after the first charging at −5 °C. The test conditions were one charge to 5 mV with a current density of 0.1 mA cm^{-2}, and holding at 5 mV. The natural graphite showed an interlayer distance, $d_{(0\,0\,2)}$, of 3.353 Å. Lithium ions intercalated within the graphite to form lithium–graphite intercalation compounds (Li–GICs) [30,31]. The staging phenomenon of the intercalated layer is a characteristic, and important, property of GICs. The mechanism of lithium intercalation into graphite has been studied using X-ray diffraction; the stage structure changes from higher to lower stages during the electrochemical intercalation of lithium. Graphite allows lithium intercalation up to a composition of LiC$_6$ at the first stage. NG showed a Li peak at $2\theta = 52.23°$ with a mixture of LiC$_6$ at $2\theta = 24.41°$ and LiC$_{12}$ at $2\theta = 25.61°$, corresponding to the first and second stages, respectively. The formation of LiC$_{12}$ was greater than LiC$_6$, indicating difficulty of lithium intercalation within the graphite layers when the cycling was conducted at a temperature low enough to reduce the mobility of the lithium ions. NC-10 graphite showed a smaller Li-metal peak with full formation of LiC$_6$ after the first charging at −5 °C. Films formed by the reduction of the electrolyte on the carbon-coated graphite could have had improved effectiveness when compared with those in the original natural graphite.

The carbon coating of graphite could improve the safety of lithium ion batteries through its enhancement of the diffusion of lithium ions into the graphite. The lithium ions potentially form components different from those formed during cycling in the absence of carbon coating. Carbon coating can suppress metal deposition on the surface of the graphite and enhance intercalation to aid the formation of LiC$_6$.

4. Conclusion

The electrochemical performance of 10 wt.% carbon-coated graphite (NC-10) at −5 °C was compared with that of natural graphite. Charge/discharge curves showed that NC-10 graphite had a higher capacity than NG; its voltage plateaus were at lower voltages. *Ex-situ* XRD measured indicated the formation of first stage LiC$_6$; a weak lithium metal peak was observed. The carbon coating aided the lithium ions' intercalation and diffusion into the graphite through the production of a SEI film with a composition different from that formed during cycling in the absence of carbon coating. Carbon coating of the surface of graphite is an effective method to enhance intercalation into the formed C$_6$Li; it can also suppress metal deposition on the surface of the graphite.

References

[1] A.N. Dey, B.P. Sullivan, J. Electrochem. Soc. 117 (1970) 222.
[2] R. Fong, U. von Sacken, J.R. Dahn, J. Electrochem. Soc. 137 (1990) 2009.
[3] M. Arakawa, J. Yamaki, J. Electroanal. Chem. 219 (1987) 273.
[4] H. Nakamura, H. Komatsu, M. Yoshio, J. Power Sources 62 (1996) 219.
[5] C. Wangm, H. Nakamura, H. Komatsu, M. Yoshio, J. Power Source 74 (1998) 142.
[6] H. Yoshitake, K. Abe, T. Kitakura, J.B. Gong, Y.S. Lee, H. Nakamura, M. Yoshio, Chem. Lett. 32 (2003) 134.
[7] K. Abe, H. Yoshitake, T. Kitakura, T. Hattori, H. Wang, M. Yoshio, Electrchim. Acta 49 (2004) 4613.
[8] G.H. Wrodnigg, J.O. Besenhard, M. Winter, J. Electrochem. Soc. 146 (1999) 470.
[9] H. Ota, K. Shima, M. Ue, J. Yamaki, Electrochim. Acta 49 (2004) 565.
[10] C. Yoon, H. Kim, S.M. Oh, J. Power Sources 94 (2001) 68.
[11] H.L. Zhang, S.H. Liu, F. Li, Carbon 44 (2006) 2212.
[12] H. Nozaki, K. Nagaoka, K. Hoshi, N. Ohta, M. Inagaki, J. Power Sources 194 (2009) 486.
[13] M. Yoshio, H. Wang, K. Fukuda, Y. Hara, Y. Adachi, J. Electrochem. Soc. 147 (2000) 1245.
[14] H. Wang, M. Yoshio, J. Power Sources 93 (2001) 123.
[15] M. Yoshio, H. Wang, K. Fukuda, Angew. Chem. Int. Ed. 42 (2003) 4203.
[16] M. Yoshio, H. Wang, K. Fukuda, T. Umeno, T. Abe, Z. Ogumi, J. Mater. Chem. 14 (2004) 1754.
[17] M.C. Smart, B.V. Ratnakuma, S. Surampudi, J. Electrochem. Soc. 146 (1999) 486.
[18] C.-K. Huang, J.S. Sakamoto, J. Wolfenstine, S. surampudi, J. Electrochem. Soc. 147 (2000) 2893.
[19] H.-P. Lin, D. Chua, M. Salomon, H.-C. Shiao, M. Hendrickson, E. Plichta, S. Slane, Electrochem. Solid-State Lett. 4 (2001) A71.
[20] S.S. Zhang, K. Xu, T.R. Low, Electrochim. Acta 48 (2002) 241.
[21] E.J. Plichta, W.K. Behl, J. Power Sources 88 (2000) 192.
[22] H.-C. Shiao, D. Chua, H.-P. Lin, S. Slane, M. Salamon, J. Power Sources 87 (2000) 167.
[23] S.S. Zhang, K. Xu, T.R. Jow, Electrochim. Acta 49 (2004) 1057.

[24] S. Herreyro, O. Huchet, S. Barussean, F. Perton, J.M. Bodet, Ph. Biensan, J. Power Sources 97–98 (2001) 576.
[25] H. Honbo, K. Takei, Y. Ishii, T. Nishida, J. Power Sources 189 (2009) 337.
[26] G. Park, H. Nakamura, Y. Lee, M. Yoshio, J. Power Sources 189 (2009) 602.
[27] M. Sphar, H. Wilhelm, F. Joho, J. Panitz, J. Wambach, P. Novak, N. Dupont-Pavlovsky, J. Electrochem. Soc. 149 (2002) A960.
[28] W. Kohs, H.J. Santner, F. Hofer, H. Schrottner, J. Doninger, I. Barsukov, H. Buqa, J.H. Albering, K.-C. Moller, J.O. Besenhard, M. Winter, J. Power Sources 119–121 (2003) 528.
[29] J.R. Dahn, Phys. Rev. B44 (1991) 9170.
[30] R. Yazami, D. Grerard, J. Power Sources 39 (1993) 43–44.
[31] T. Ohzuku, Y. Iwakoshi, K. Sawai, J. Electrochem. Soc. 140 (1993) 2490.